Journal of Hazardous Materials B118 (2005) 185–195

Journal of Hazardous Materials

www.elsevier.com/locate/jhazmat

A SEM and X-ray study for investigation of solidified/stabilized arsenic–iron hydroxide sludge

Tanapon Phenrat[a], Taha F. Marhaba[b,*], Manaskorn Rachakornkij[c]

[a] *National Research Center for Environmental and Hazardous Waste Management, Chulalongkorn University, Bangkok, Thailand*

[b] *Associate Professor and Director, New Jersey Applied Water Research Center, New Jersey Institute of Technology, University Heights, Newark, New Jersey, USA*

[c] *Department of Environmental Engineering, Faculty of Engineering, Chulalongkorn University, Bangkok, Thailand*

Received 23 July 2004; received in revised form 21 October 2004; accepted 27 October 2004
Available online 25 December 2004

Abstract

Despite the fact that the solidification/stabilization of arsenic containing wastes with Portland cement and lime has an extensively documented history of use, the physical and chemical phenomena as a result of the interaction between arsenic and cement components have not been fully characterized. The study investigates the behavior of synthesized arsenic–iron hydroxide sludge, the by-product of arsenic removal by coagulation with ferric chloride, in solidified/stabilized matrices as well as its binding mechanisms by exploring the cementitious matrices in the micro-scale by scanning electron microscopy equipped with energy dispersive X-ray spectrometer (SEM-EDS). It was revealed that arsenic can be chemically fixed into cementitious environment of the solidified/stabilized matrices by three important immobilization mechanisms; sorption onto C–S–H surface, replacing SO_4^{2-} of ettringite, and reaction with cement components to form calcium–arsenic compounds, the solubility limiting phases.

Keywords: Arsenic–iron hydroxide sludge; Microstructure; SEM-EDS; Immobilization mechanism; Solidification/stabilization

1. Introduction

The unavoidable and unwanted by-product of arsenic removal by coagulation with ferric chloride is the large amount of iron hydroxide sludge with elevated arsenic content. If the sludge becomes classified as hazardous, solidification/stabilization (S/S) technology is usually used to transform potentially hazardous arsenic containing waste into less hazardous or non-hazardous solid waste before land disposal or waste utilization [1]. The binders and reagents generally used in the solidification and stabilization process of arsenic are cement, fly ash, lime, sulfur, phosphate, and pH adjustment agents. Of all these additives, the most frequently used binders for the S/S of arsenic are Portland cement and lime because they are inexpensive and have an extensively documented history of use [1–9].

Despite the fact that solidification/stabilization has emerged and been applied to cope with various types of wastes ranging from radioactive to biological for several decades, the physical and chemical phenomena as a result of the interaction between the priority metal pollutants such as arsenic with cement components, have not been fully characterized. The objective of the present study is to investigate the behavior of arsenic in solidified/stabilized matrices as well as its binding mechanisms by exploring the cementitious

* Corresponding author. Tel.: +973 642 4599; fax: +973 596 5790.
E-mail address: marhaba@adm.njit.edu (T.F. Marhaba).

0304-3894/$ – see front matter © 2004 Elsevier B.V. All rights reserved.
doi:10.1016/j.jhazmat.2004.10.019

matrices in the micro-scale by scanning electron microscopy equipped with energy dispersive X-ray spectrometer (SEM-EDS).

2. Materials and methods

2.1. Materials

2.1.1. Reagents and glassware

All chemicals were reagent grade and were used without further purification. All solutions were prepared with water purified by reverse osmosis and deionized using ELGA Purelab system. All glassware was cleaned by soaking in 10% HNO_3 and rinsed several times with deionized (DI) water. The arsenite stock solution was prepared from the sodium arsenite, $NaAsO_2$, (UNIVAR) dissolved in 1% (v/v) trace metal grade HCl (Scharlau). The Fe(III) stock solution was prepared from ferric chloride hexahydrate, $FeCl_3{\cdot}6H_2O$ (Riedel-deHaën) dissolved in 1% (v/v) trace metal grade HCl.

2.1.2. Arsenic–iron hydroxide sludge

The arsenic–iron hydroxide sludge used in this study was synthesized at pH 7 by simulating the chemical reaction between ferric chloride and arsenite in the arsenic removal process by coagulation/co-precipitation. However, according to the FT-IR analysis of the sludge in the previous study [10], it was found that both arsenite and arsenate were present in the sludge sample. The sludge was not only dewatered by vacuum filtration but also dried by heat at 105 °C before S/S. As-to-Fe ratio of the sludge was around 0.153. The raw sludge was classified as hazardous waste due to the fact that arsenic concentration in leachate according the toxicity characteristic leaching procedure (TCLP) was 20.70 mg/l, 20 times higher than the acceptable limit according to the newly revised maximum contamination level (MCL) of the United States, which is 1 mg/l. Other physical properties of the sludge are shown in Table 1.

Table 1
Some chemical and physical characteristics of the binders and the sludge

	SiO_2	Al_2O_3	Fe_2O_3	CaO	$Ca(OH)_2$
Chemical composition of binder materials (wt.%)					
Portland cement	22	6	3	65	–
Hydrated lime	–	–	–	–	96.0

	Cement	Lime	Dried sludge
Physical properties of binders and sludge			
Specific gravity	3.15	2.24	2.49[a]
Absorption (%)	–	–	54.34[b]

[a] Specific gravity of the sludge was tested under saturated surface dry condition (SSD) simulated by pouring water through the sludge lying on filter and allowing water to freely flow through the sludge until the sludge was in SSD condition in which no water could be sorbed or desorbed anymore.
[b] Adsorption of the sludge was tested in the same manner as specific gravity.

2.1.3. Portland cement

The Elephant brand ASTM Type-I Portland cement according to ASTM C150-95 manufactured by the Siam Cement Company Ltd., Bangkok, Thailand was used throughout the experiments. The chemical compositions and physical properties of the Portland cement are shown in Table 1.

2.1.4. Water

Ordinary tap water meeting World Health Organization drinking water standards was used for all mixes.

Table 2
Mixture proportion of the solidified/stabilized sample

Notation	Mixture proportion (kg/m^3)				Ratio		
	Water (w)	Cement (c)	Lime (l)	SSD sludge (s)	$w/(l+c)$	$s/(l+c)$	$l/(l+c)$
SW4-S25-L00	488.72	1221.88	0.00	305.47	0.40	0.25	0.00
SW4-S25-L04	459.73	689.75	459.73	287.53	0.40	0.25	0.40
SW6-S25-L00	589.00	981.77	0.00	245.40	0.60	0.25	0.00
SW6-S25-L04	560.80	560.80	374.03	233.71	0.60	0.25	0.40
SW9-S25-L00	681.58	759.27	0.00	190.62	0.90	0.25	0.00
SW9-S25-L04	656.91	437.94	293.14	183.57	0.90	0.25	0.40

Table 3
Semi quantitative EDS analysis of interaction between arsenic and various hydration by-products and excluding calcium–arsenic compounds

Sample	Illustrated in figure	Age (days)	Atomic (%)												Note
			Ca	Si	O	Fe	As	S	Na	Mg	Al	K	C	Cl	
SW9-S25-L00	1	7	10.70	7.09	71.88	0.66	1.19	-	5.31	0.94	0.98	1.00	–	0.25	Ca:Si = 1.51
SW6-S25-L04	3	28	11.93	4.96	66.70	1.36	2.06	0.01	0.90	–	1.93	0.22	9.74	0.19	
SW4-S25-L00	4	7	18.60	10.12	64.63	0.71	0.30	0.29	1.83	0.79	1.78	0.52	–	0.43	
SW4-S25-L04	7	7	18.59	1.62	74.06	2.44	0.13[a]	–	–	0.31	2.84	–	–	–	
Sw9-S25-L04	8	7	18.62	0.39	73.37	0.16	0.03[a]	–	0.54	0.17	5.00	0.05	–	1.68	
SW6-S25-L04	9	7	30.73	2.11	65.04	0.08[a]	0.1[a]	–	0.86	0.23[a]	0.42	0.23	–	0.20	

[a] $<2\Sigma$.

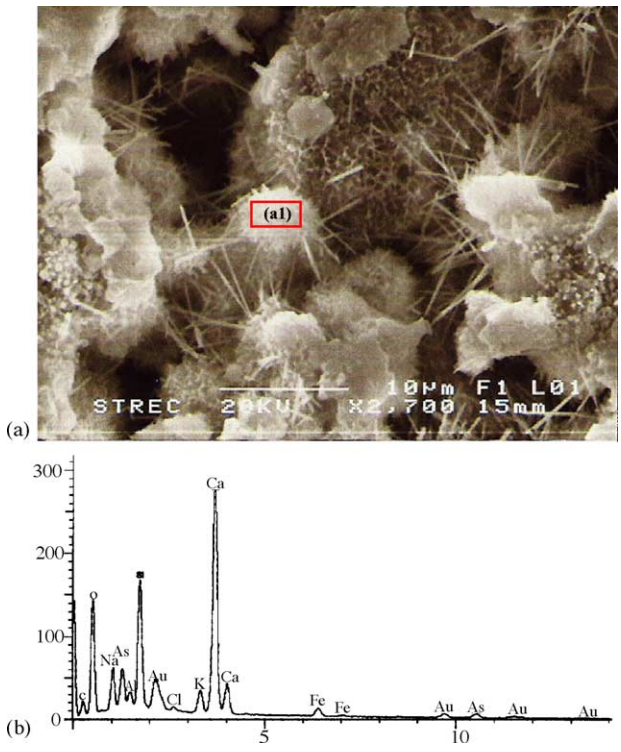

Fig. 1. (a) SEM photographs of SW9-S25-L00 at the age of 7 days; (b) EDS spectrum focusing on C—S—H microstructure (a1) to investigate arsenic sorption potential.

2.2. Methods

Six sets of cement paste of which mixtures are shown in Table 2 were manually mixed with a plastic spatula until appearing homogeneous. Then, the pastes were casted into

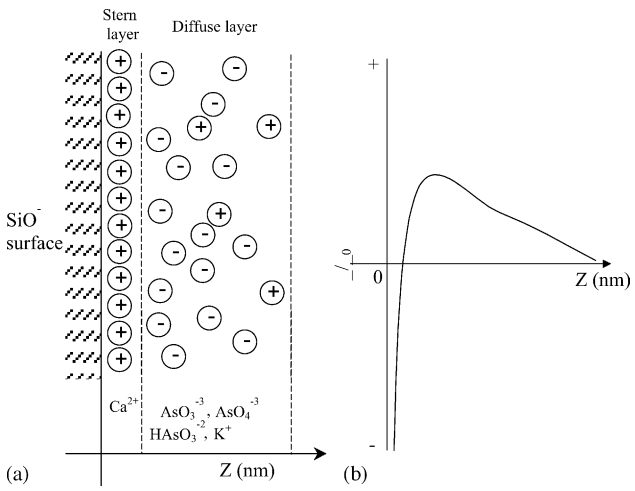

Fig. 2. (a) Overcompensation of the surface charge by Ca^{2+} hypothesis for sorption of arsenic oxyanions onto C—S—H surface in cement porewaters (adapted from Jösson et al. [13], Park and Batchelor [14], and Stumm and Morgan [15]); (b) schematic representation of the curve indicating the total accumulated charge including surface charge (SiO^-), the counterion (Ca^{2+}), and the co-ions (AsO_3^{3-}, AsO_4^{3-}, $HAsO_3^{2-}$, and K^+) up to a distance Z from the surface (adapted from Jösson et al. [13]).

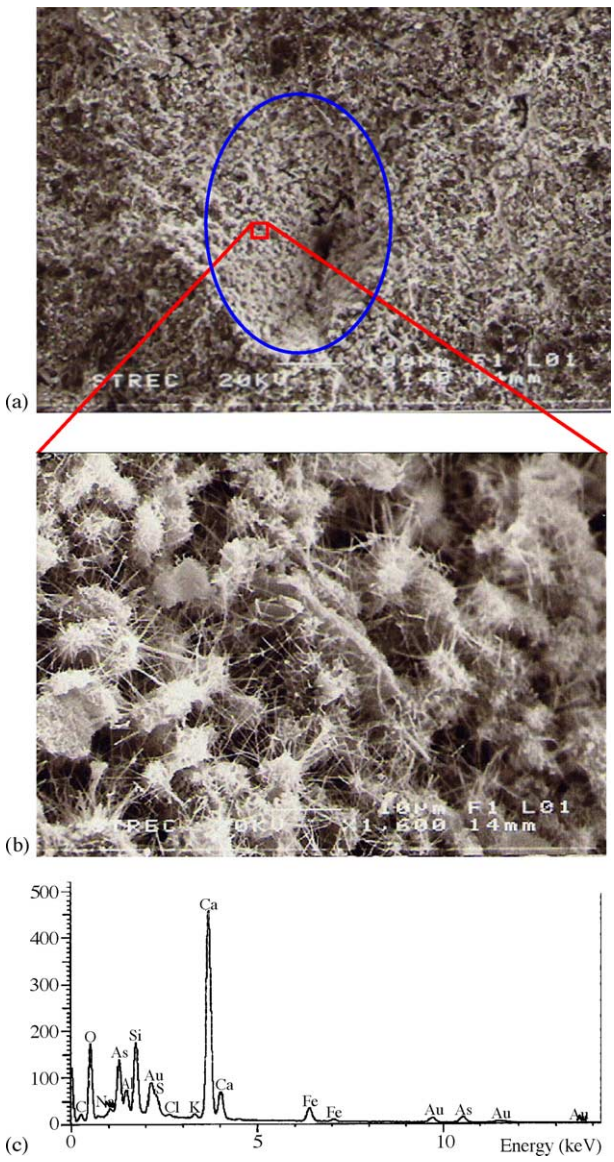

Fig. 3. (a) SEM photographs of SW6-S25-L04 at the age of 7 days focusing on the hole once encapsulating the arsenic containing sludge; (b) SEM photographs zooming on microstructures at the interface of the sludge and cement; and (c) EDS spectrum focusing on ettringite microstructure to investigate arsenic immobilization potential.

5 mm diameter plastic tubes. By the age of 3, 7, 14, and 28 days, respectively, the samples were cross-sectionally cracked, coated with gold, and their microstructures were observed by a JEOL JSM 6400 Scanning Electron Microscopy. Moreover, an EDS, Link^{isis} Series, was used to

Table 4
Formation of hydration products from $3CaO{\cdot}Al_2O_3$ [17]

Ca $SO_4{\cdot}H_2O/3CaO{\cdot}Al_2O_3$ molar ratio	Hydration products formed
3.0	Ettringite
3.0–1.0	Ettringite + monosulfoaluminate
1.0	Monosulfoaluminate
<1.0	Monosulfoaluminate solid solution
0.0	Hydrogarnet

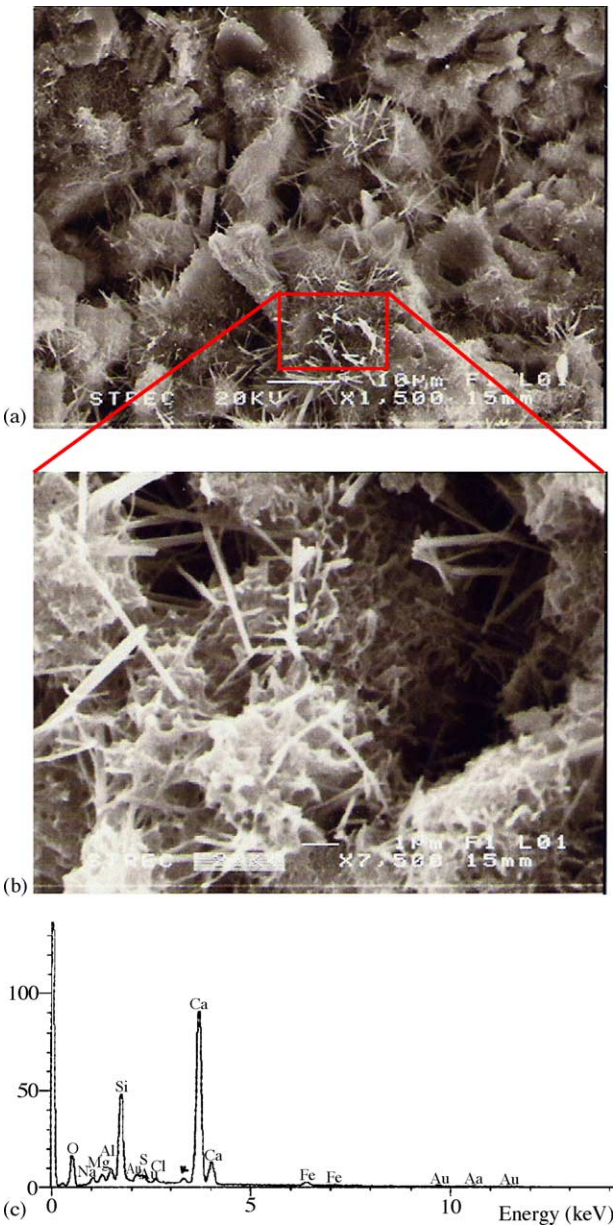

Fig. 4. (a) SEM photographs of SW4-S25-L00 at the age of 7 days; (b) SEM photographs zooming on needle-like microstructure of ettringite; and (c) EDS spectrum pointing at ettringite microstructure to investigate arsenic immobilization potential.

identify various microstructures in these solidified waste forms by determining their elemental compositions.

3. Results and discussions

3.1. Application of SEM-EDS for microstructural analysis of the solidified/stabilized arsenic–iron hydroxide sludge

The morphology of each sample listed in Table 2 was analyzed at 3, 7, 14, and 28 days using SEM-EDS. This section organizes and presents the results according to the type of hydration by-product.

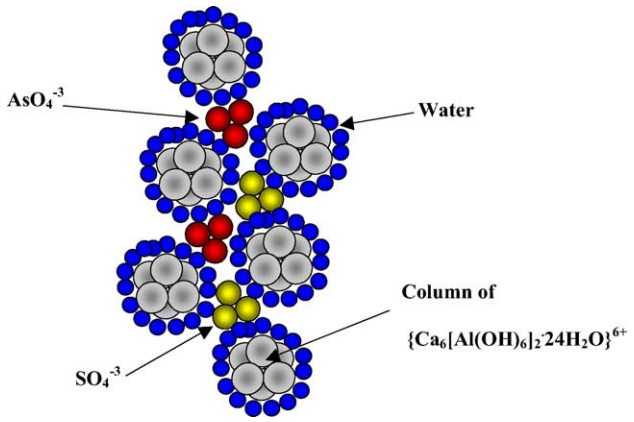

Fig. 5. Structure of ettringite of which some sulfate ions are substituted by arsenate oxyanion (adapted from Myneni et al. [16]).

3.1.1. Calcium silicate hydrate (C–S–H)

Approximately formulated by Eqs. (1) and (2), the hydration reactions of tricalcium silicate and dicalcium silicate, two major components of Portland cement, are origins of C–S–H. The formula $3CaO \cdot 2SiO_2 \cdot 3H_2O$ is only

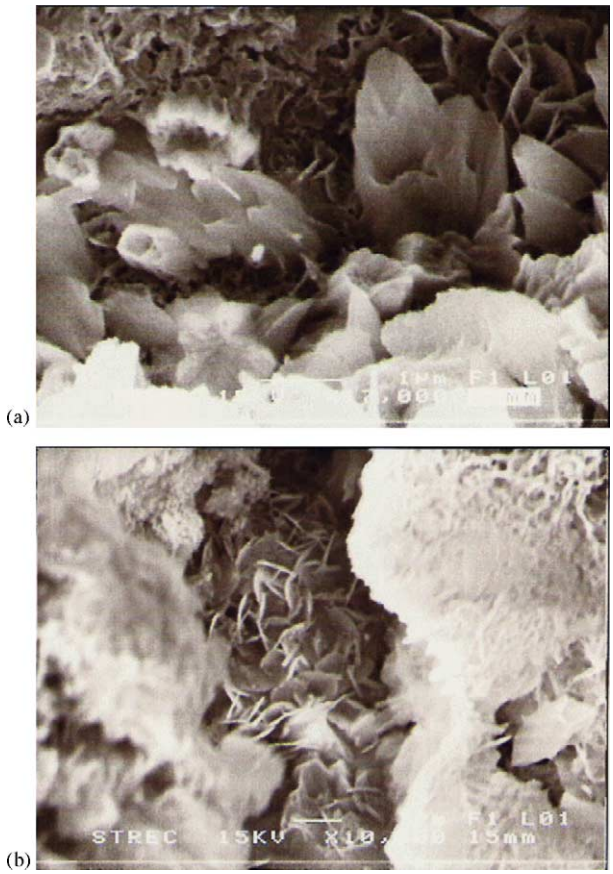

Fig. 6. (a) SEM photographs of SW4-S25-L04 at the age of 3 days; (b) SEM photographs of SW6-S25-L04 at the age of 14 days. Both focus on rosette-like morphology of monosulfoaluminate.

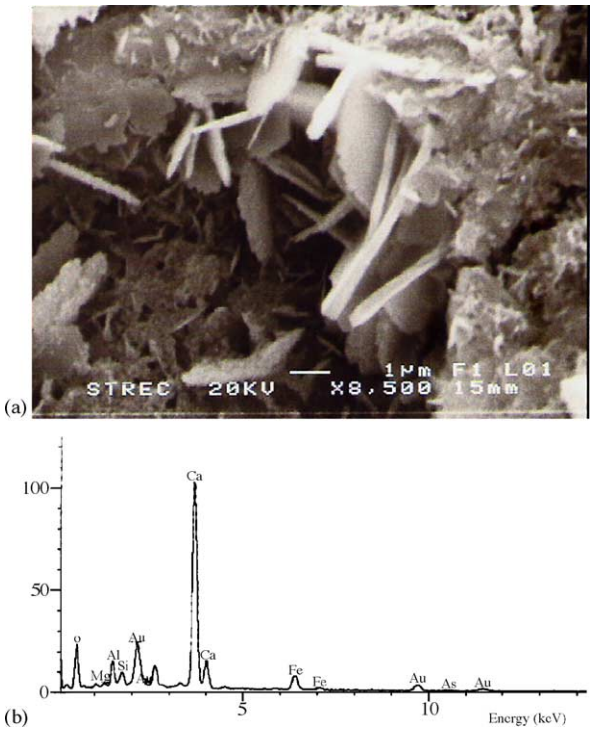

Fig. 7. (a) SEM photographs of SW4-S25-L04 at the age of 7 days focusing on hexagonal-plate morphology of hydrated calcium aluminate/ferrite; (b) EDS spectrum pointing at hexagonal-plate structure to investigate arsenic immobilization potential.

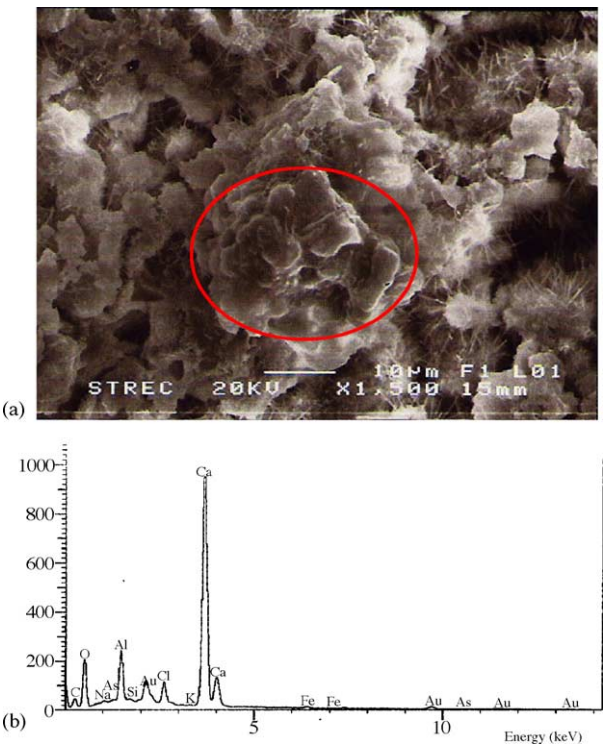

Fig. 8. (a) SEM photographs of SW9-S25-L04 at the age of 7 days focusing on ill-defined morphology of hydrated calcium aluminate; (b) EDS spectrum pointing at ill-defined structure to investigate arsenic immobilization potential.

an approximate description, as the stoichiometry is quite variable. The $CaO:SiO_2$ molar ratio can vary from 0.8 to 2.0 depending on many factors: age of the paste, temperature of hydration, and water-to-cement ratio [11].

$$\underset{\text{ticalcium silicate}}{2(3CaO \cdot SiO_2)} + 6H_2O \underset{\text{water}}{\rightleftarrows} 3CaO \cdot 2SiO_2 \cdot 3H_2O + \underset{\text{calcium hydroxide}}{3Ca(OH)_2} \quad (1)$$

$$\underset{\text{dicalcium silicate}}{2(2CaO \cdot SiO_2)} + 4H_2O \underset{\text{water}}{\rightleftarrows} 3CaO \cdot 2SiO_2 \cdot 3H_2O + \underset{\text{calcium hydroxide}}{Ca(OH)_2} \quad (2)$$

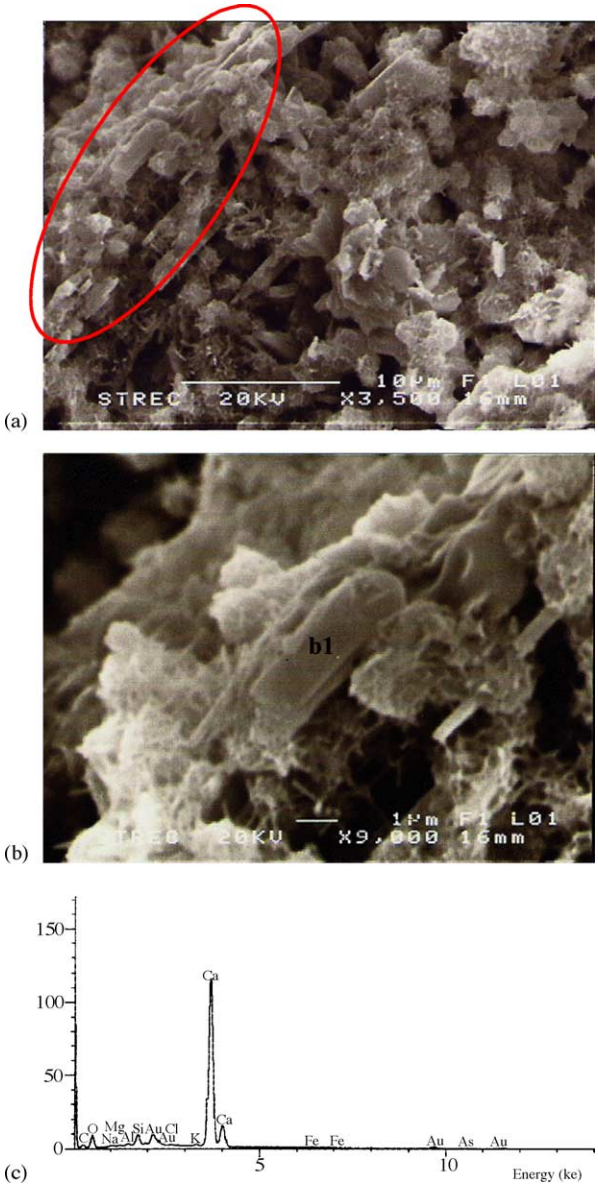

Fig. 9. (a) SEM photograph of SW6-S25-L04 at the age of 7 days; (b) the same SEM photograph zooming on $Ca(OH)_2$ microstructures; and (c) EDS spectrum pointing on b1 representing $Ca(OH)_2$ to investigate arsenic immobilization potential.

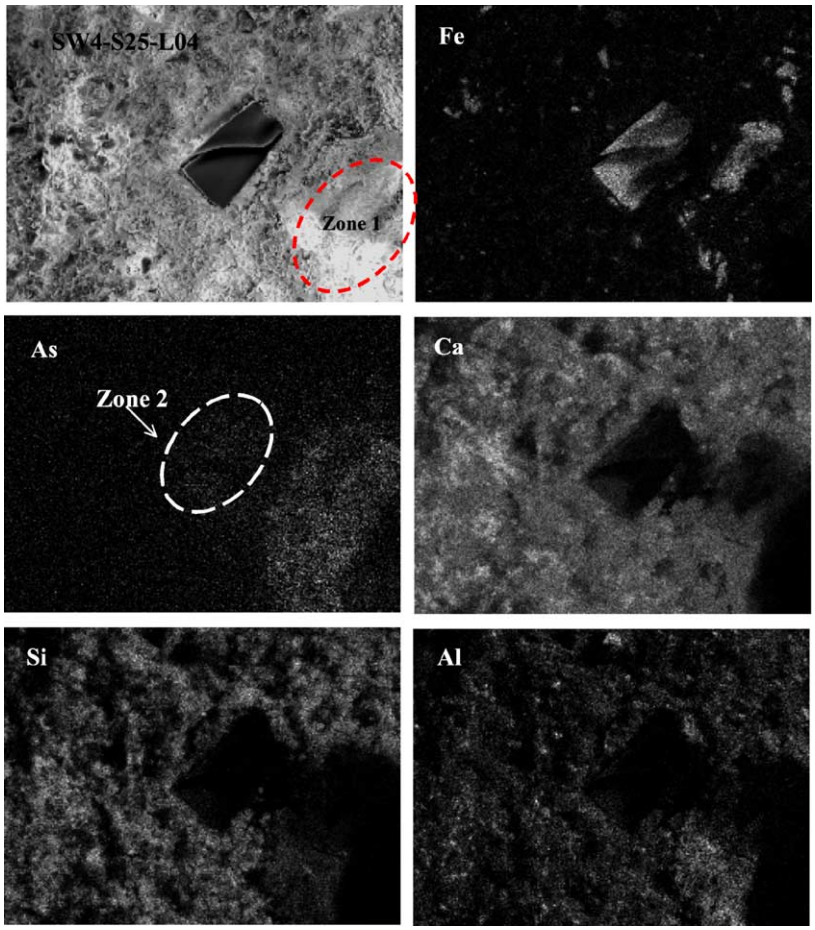

Fig. 10. The X-ray dot maps of SW4-S25-L04 at the age of 7 days comparing arsenic distribution between Zone 1 where arsenic desorbing from the sludge is located and Zone 2 where arsenic remaining at the surface of the sludge is located.

This hydration by-product not only has a direct influence on strength of the solidified matrices but also potentially has a hand in waste immobilization. As shown in Fig. 1 as well as in Table 3, it is evident that arsenic was sorbed on C–S–H microstructures. Sorption potential of metals on C–S–H is supposed to be controlled by an important characteristic of C–S–H. The fact that C–S–H has a very high specific surface area with irregular hydrogen bonding can facilitate sorption of both water and other alien ions such as metal ions [12].

Measured by N_2 sorption, the specific surface of C–S–H is in the range of 10–50 m^2/g [12]. The outer surfaces of the C–S–H nanoparticles are made of silicate with SiOH surface groups. At high pH of the cementitious system (pH 10–13), these SiOH surface groups react with OH^- ions of the solution to give negatively charged SiO^- groups [13]. At the same pH, arsenic oxyanion is also supposed to be negatively charged, so in contrast to the experimental result shown in Fig. 1 as well as in Table 3, sorption of negatively charged arsenic oxyanion onto SiO^- groups of C–S–H is unlikely unless other phenomena lead to a charge reversal.

In the cementitious system with the presence of Ca^{2+}, the charge reversal of C–S–H is possible. According to the principle of interface chemistry as well as the recent literature

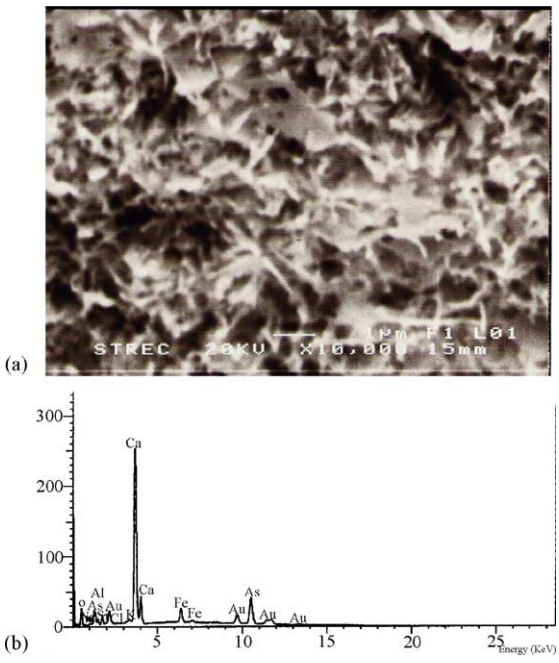

Fig. 11. (a) SEM photograph of SW4-S25-L04 at the age of 7 days focusing on one of the possible calcium–arsenic compound; and (b) its EDS spectrum.

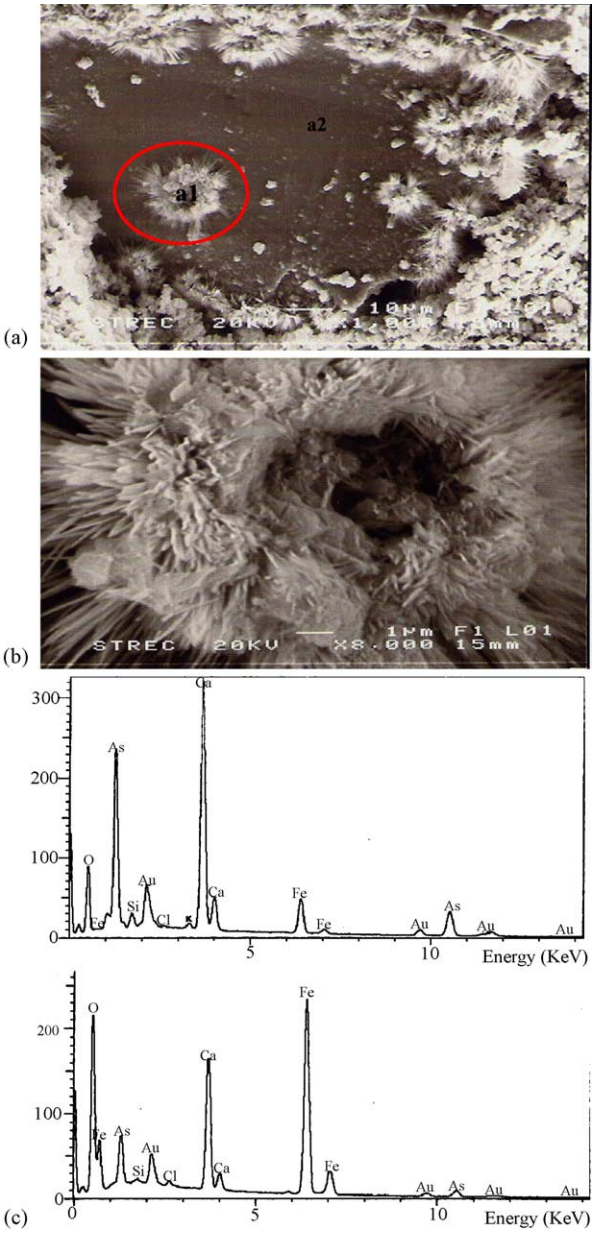

Fig. 12. (a) SEM photograph of SW4-S25-L04 at the age of 28 days; (b) the same SEM photograph zooming on another calcium–arsenic compound; and (c) EDS spectrum pointing on (a1) the calcium–arsenic compound; and (d) EDS spectrum pointing on (a2) the arsenic-containing sludge. Comparing (c) and (d) is a clear evidence of arsenic transformation from the sludge to calcium–arsenic compound.

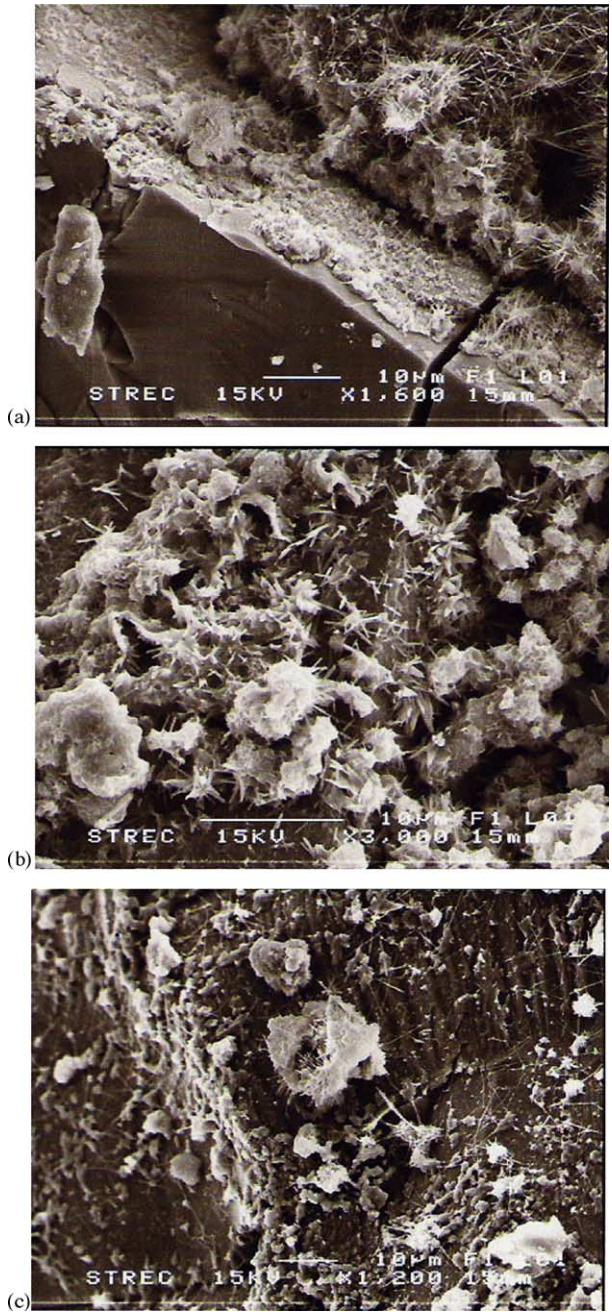

Fig. 13. SEM photograph illustrating several hydrated phases interfacing with the arsenic-iron sludge at the early age (3 days) of (a) SW4-S25-L00; (b) SW6-S25-L04; and (c) SW9-S25-L00. It should be noted that there are no calcium–arsenic compound shown in Fig. 12.

[13], three assumptions proposing a charge reversal could be adapted to describe the sorption of arsenic oxyanion onto C–S–H nanoparticles. The first possibility is the formation of inner-sphere complex, where Ca^{2+} loses some of its hydration water and marks a direct ionic bond to the SiO^- surface site as illustrated in Eq. (3). Another possibility is the formation of a solvent separated ion coordinator as illustrated in Eq. (4). The last possibility is the overcompensation of SiO^- surface charges by accumulated Ca^{2+} counterions. The amount of accumulated counterions may overcompensate the surface charges, and at the larger distance there apparent positive charges are supposed to be compensated by a concentration of negatively charged ions in the system [13] such as arsenic oxyanions in this case. This is believed to facilitate adsorption of arsenic oxyanions onto C–S–H surface. Shown in Fig. 2 is the illustration of this assumption. The extent of overcompensation depends on the availability of Ca^{2+}. The accumulated charges increase

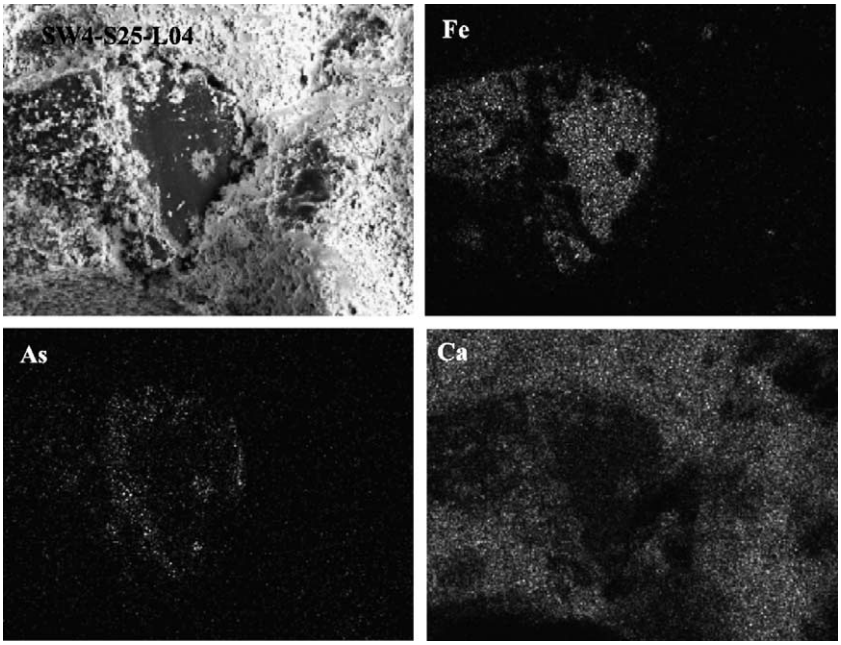

Fig. 14. The X-ray dot maps of SW4-S25-L04 at the age of 28 days focusing on the arsenic compound formed at the interface zone. It is evident that that density of arsenic on the surface of the sludge is less than that in calcium–arsenic compound. Therefore, transformation of arsenic from surface of the sludge to calcium–arsenic compound is supposed to take place.

with the amount of Ca^{2+} in the system [13].

$$SiO^{-} \cdots HOH + HOH \cdots Ca^{2+} \rightarrow SiCa^{+} + 2HOH \quad (3)$$

$$SiO^{-} \cdots HOH + HOH \cdots Ca^{2+} \rightarrow SiO \cdots HOH \cdots Ca^{2+} + HOH \quad (4)$$

Although these three assumptions are different from one another, one thing that all have in common is the fact that Ca^{2+} plays a vital role in the charge reversal. This is in good agreement with the relationship between surface charge and Ca:Si ratio suggested by Glasser [12]. He revealed that the surface charge of C–S–H varies with its composition; Ca-rich C–S–H has a positive surface charge and tends to sorb anions such as oxyanions in alkaline condition. In contrast, as Ca:Si ratio decreases, the positive surface charge gradually lessens, passing through zero at a Ca:Si ratio of 1.2 and eventually becoming negative at lower ratios. According to this assumption, as shown in Table 3 that Ca:Si ratio of C–S–H structure in Fig. 1 is 1.51, the surface charge of this C–S–H structure is supposed to be positive, and arsenic oxyanion with negative charge trends to sorb on them.

3.1.2. Ettringite, monosulfoaluminate, and other hydrated calcium aluminates/ferrite

Figs. 3 and 4 illustrate the needle-like microstructure of ettringite, a hydration by-product of tricalcium aluminate in the presence of sulfate ions as formulated by Eq. (5). It is well known that this hydration by-product can reduce the strength of the solidified matrices; nevertheless, ettringite was suggested to have the potential to immobilize oxyanions especially As(V) ions [16].

$$\underset{\text{tricalcium aluminate}}{3CaO \cdot Al_2O_3} + \underset{\text{gypsum}}{3CaSO_4} + \underset{\text{water}}{32H_2O} \rightleftarrows \underset{\text{ettringite}}{Ca_6Al_2(SO_4)_3(OH)_{12} \cdot 26H_2O} \quad (5)$$

The ettringite crystal structure consists of columns of $\{Ca_6[Al(OH)_6]_2 \cdot 24H_2O\}^{6+}$ with the intercolumn space (channels) occupied by anions such as SO_4^{2-}, and H_2O molecules. The column H_2O molecules form H-bonds with channel ions and hold the columns together through electrostatic interaction. Thus, oxyanion immobilization by ettringite results in channel substitution by replacing SO_4^{2-} or H_2O and/or formation of complexes with surface functional groups by replacing OH or H_2O [16] as illustrated in Fig. 5.

It should be noted that although having the same structure, ettringite of SW6-S25-L04 and SW4-S25-L00 retained different amounts of arsenic, which were 2.06 and 0.3% atomic weight, respectively. The sharp distinction of these two samples, which might be responsible for the different retention of arsenic, is arsenic availability. For example, ettringite of SW6-S25-L04 was formed at interface between cement paste and the arsenic containing sludge, so there was abundance of arsenic to be crystallochemically incorporated by ettringite. In contrast, ettringite of SW4-S25-L00 was relatively far from the sludge; limited amount of arsenic might available there. Therefore, even though crystallochemically incorporating all arsenic available, ettringite in SW4-S25-L00 might not reach its maximum arsenic immobilization capacity.

Ettringite is a stable hydration product only while there is an ample supply of sulfate available, as shown in Table 4

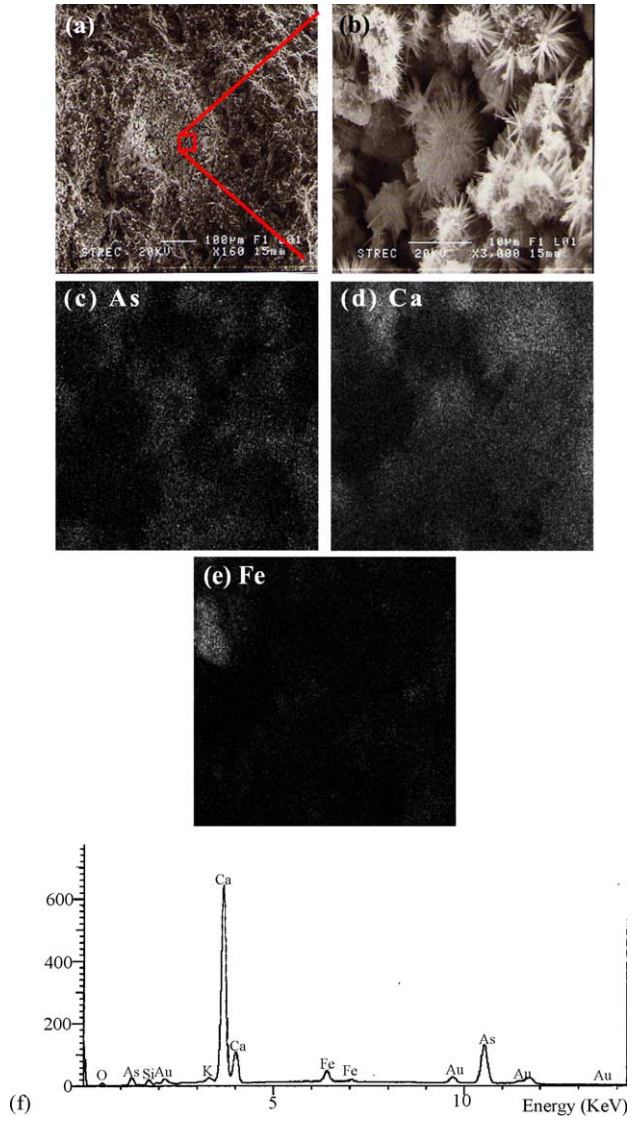

Fig. 15. (a) SEM photograph of SW4-S25-L00 at the age of 28 days, (b) the same SEM photograph zooming on grass leaf-like microstructures of the calcium–arsenic compound, (c), (d) as well as (e) the X-ray dot maps of (b) focusing on As, Ca and Fe respectively, and (f) EDS spectrum pointing on the calcium–arsenic compound to investigate arsenic immobilization potential.

[17]. If sulfate is all consumed before $3CaO{\cdot}Al_2O_3$ or $4CaO{\cdot}Al_2O_3$. Fe_2O_3 has completely hydrated, ettringite tends to transform to another calcium sulfoaluminate hydrate containing less sulfate, simply called monosulfoaluminate [17] as formulated by Eq. (6). When first formed monosulfoaluminate tends to form clusters or rosettes of irregular plates. Later, it tends to grow into well-developed, but very thin, hexagonal plates.

$$Ca_6Al_2(SO_4)_3(OH)_{12} \cdot 26H_2O + 2(3CaO \cdot Al_2O_3) + 4H_2O \rightleftarrows 3(3CaO \cdot Al_2O_3 \cdot CaSO_4 \cdot 12H_2O) \quad (6)$$

Fig. 6 illustrates SEM photographs of monosulfoaluminate found in this study. Unfortunately, EDS could not be applied to reliably investigate their compositions because they were located in a cavity obstructed by several hydrated structures. However, theoretically, monosulfoaluminate, like ettringite, should be able to immobilize arsenic due to the fact that it also consists of SO_4^{2-} which arsenic ion can replace. This assumption is in good agreement with recent study of Baur and Johnson [18], who investigated sorption of selenite and selenate-oxyanions of which several properties correspond to that of arsenic and concluded that selenite and selenate were effectively sorbed by cement where monosulfate was present in significant amount.

According to both the available results of this study and the literature, sulfate substitute is one of the important binding mechanisms of arsenic in cementitious environment. This assumption can be confirmed by considering other hydrated calcium aluminates or ferrites structures formed without SO_4^{2-} shown in Figs. 7 and 8 as well as Table 3. It is found that insignificant amount of arsenic was detected in such structures.

3.1.3. *Calcium hydroxide [$Ca(OH)_2$]*

Although produced from $2CaO{\cdot}SiO_2$ and $3CaO{\cdot}SiO_2$ during hydration reaction like C–S–H, $Ca(OH)_2$, a well crystallized material with a definite stoichiometry, appears to have little potential for both sorption and crystallochemical incorporation of arsenic. As shown in Fig. 9 and Table 3, only insignificant amount of arsenic is supposed to be either sorbed

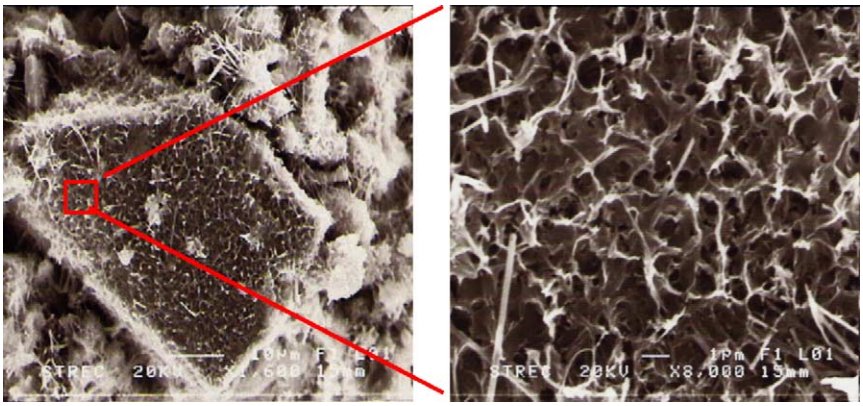

Fig. 16. (a) SEM photograph of SW4-S25-L00 at the age of 28 days and (b) the same SEM photograph zooming on the thin layer covering the sludge.

Table 5
Summation of all the possible calcium–arsenic compounds observed in this study together with their morphologies and compositions by EDS

Sample	Age (days)	Atomic (%)										Ca/As	Morphology
		Ca	Si	O	Fe	As	Na	Mg	Al	K	Cl		
SW4-S25-L04	7	25.24	2.01	44.28	3.25	22.73	0.44	0.16	1.30	0.43	0.17	1.11	Leafy crystals
SW4-S25-L04	28	16.54	1.56	67.26	3.89	10.31	–	–	–	0.29	0.14	1.60	Grass leaf-like
SW4-S25-L00	28	38.87	1.96	10.5	3.35	44.68	–	–	–	0.65	–	0.87	Grass leaf-like

or crystallochemical incorporated into $Ca(OH)_2$. This may be a result of that the surface of $Ca(OH)_2$ does not have positive charge like that of C–S–H, nor does it contain SO_4^{2-} for arsenic to substitute.

3.1.4. Calcium–arsenic compounds

While crystallized $Ca(OH)_2$ discussed in the previous section seems inefficient in binding arsenic by both sorption and lattice inclusion, calcium ion saturating in pore fluid from both hydration and addition of powder of hydrated lime as an additive seems considerably beneficial for arsenic immobilization by reacting with arsenic to form calcium–arsenic compounds, solubility limiting phases.

Arsenic is supposed to concentrate both at the surface of the sludge encapsulated by cement matrix and to distribute in aqueous phase of pore structure as shown in Fig. 10. Therefore, calcium-to-arsenic ratio at the interface between cement paste and the sludge may differ from that between calcium ion and arsenic oxyanion dissolved in pore water. For this reason, as mentioned in the previous [1,10] as well as in literature [6], it is possible that more than one type of calcium–arsenic compounds is formed in such environment.

Fig. 11 illustrates one of the possible calcium–arsenic compounds forming in the solidified/stabilized matrices. This compound was found in zone 1 in Fig. 10, so it is supposed to form by precipitation between calcium and arsenic ion dissolved in pore fluid.

In contrast, Fig. 12 shows another type of calcium–arsenic compound. Unlike the calcium–arsenic compound discussed in previous paragraph, this compound was located at the interface between the cement paste and the sludge. Moreover, its grass leaf-like morphology is completely different from leafy crystals of the calcium–arsenic compound shown in Fig. 11.

The most important difference between these two calcium–arsenic compounds is the fact that the former was detected at the age of 7 days while the latter was detected at the age of 28 days. The former is supposed to be a result of the interaction between calcium ion from either hydration reaction or addition of calcium hydroxide powder and arsenic(V) desorbed due to the influence of pH discussed in the previous study [1,10]. The supporting reason of this assumption is the fact that desorption of arsenic under the influence of pH is supposed to not consume so long time. In contrast, the latter is supposed to be result of the interaction between calcium ion from either hydration reaction or/and addition of calcium hydroxide powder and desorbed arsenic(V) that was oxidized from arsenic (III) at the surface of the sludge. Oxidation of As(III) to As(V) is possible in cementitious environment because of the fact that, normally, E_h of cement pore fluid is from +100 to +200 mV. Generally, the principle electroactive species in pore fluid are believed to be oxygen dissolved in mix water and perhaps traces of sulfite, SO_3^{2-}, formed by condensation of kiln vapors which came in contact with the cement during cement clinker cooling [12]. Therefore, the oxidation may gradually take place; that is why the latter form of calcium–arsenic compound was found at the age of 28 days while it was absent at the early age as shown in Fig. 13. In addition, Fig. 14 shows the X-ray dot maps of Fig. 12 to emphasize transformation of arsenic from surface of the sludge to the calcium–arsenic compound. It is clearly seen that the density of arsenic on the surface of the sludge is less than that in calcium–arsenic compound.

In the same way, Fig. 15 illustrates the grass leaf-like morphology of the calcium arsenic compound detected at the interface between cement paste and the arsenic containing sludge. This figure is analogous to Fig. 3, but they were recorded at different ages; however, it should be noticed that, from the age of 7 days in Fig. 3 to 28 days in Fig. 15, ettringite disappeared while calcium–arsenic compound was present. This is also a good evidence of transformation of arsenic from the sludge and the formation of the calcium–arsenic compound.

In addition to the identifiable compounds discussed above, there are some abnormal morphologies observed at the interface between the sludge and cement paste. For example, shown in Fig. 16 is the thin layer of the unidentified compound supposed to be one of the calcium–arsenic compounds. This layer covered the sludge so close that EDS could not distinguish between compositions of the layer and the sludge.

4. Summary and conclusion

- The study investigated the behavior of arsenic–iron hydroxide sludge, the by-product of arsenic removal by coagulation with ferric chloride, in solidified/stabilized matrices as well as its binding mechanisms by exploring the cementations microworld by scanning electron microscopy equipped with energy dispersive X-ray spectrometer.
- Arsenic can be chemically fixed into cementations environment of the solidified/stabilized matrices by three important immobilization mechanisms;

- sorption onto C–S–H surface;
- replacing SO_4^{2-} of ettringite; and
- reaction with cement components to form calcium–arsenic compounds, the solubility limiting phases.

- Of all the three, the formation of calcium–arsenic compounds should be the most effective immobilization mechanism since, in this study, amounts of arsenic incorporated in such compounds are significantly higher than those sorbed onto C–S–H or incorporated into ettringite.
- All the possible calcium–arsenic compounds observed in this study together with their morphologies and compositions are summarized in Table 5.

Acknowledgements

This research work was funded by the National Research Center for Environmental and Hazardous Waste Management, Chulalongkorn University, Bangkok, Thailand and the New Jersey Applied Water Research Center, New Jersey Institute of Technology, Newark, NJ, USA. The authors also would like to express gratitude to the Scientific and Technological Research Equipment Center of Chulalongkorn University, especially Mr. Boonlur who gave many helpful suggestions. The assistance of Dr. Khemarath Osathaphan is also gratefully acknowledged.

References

[1] T. Phenrat, T.F. Marhaba, M. Rachakornkij, Examination of solidified and stabilized matrices as a result of the solidification and stabilization process of arsenic containing sludge with Portland cement and lime, Songklanakarin J. Sci. Technol. 26 (Suppl. 1) (2004) 65–75.

[2] V. Dutré, C. Vandecasteele, Solidification/stabilization of hazardous arsenic containing waste from a copper refining process, J. Hazard. Mater. 40 (1995) 55–68.

[3] V. Dutré, C. Vandecasteele, Solidification/stabilization of arsenic-containing waste: leach tests and behavior of arsenic in the leachate, Waste Manage. 15 (1995) 55–62.

[4] V. Dutré, C. Vandecasteele, An evaluation of the solidification/stabilization of industrial arsenic containing waste using extraction and semi-dynamic leach tests, Waste Manage. 16 (1996) 625–631.

[5] V. Dutré, C. Vandecasteele, Immobilization of arsenic in waste solidified using cement and lime, Environ. Sci. Technol. 32 (1998) 2782–2787.

[6] J.V. Bothe Jr., P.W. Brown, Arsenic immobilization by calcium arsenate formation, Environ. Sci. Technol. 33 (1999) 3806–3811.

[7] P. Palfy, E. Vircikova, L. Molnar, Processing of arsenic waste by precipitation and solidification, Waste Manage. 19 (1999) 55–59.

[8] C. Vandecasteele, V. Dutré, D. Geysen, G. Wauters, Solidification/stabilization of arsenic bearing fly ash from the metallurgical industry: immobilization mechanism of arsenic, Waste Manage. 22 (2002) 143–146.

[9] C. Jing, G.P. Korfiatis, X. Meng, Immobilization mechanisms of arsenate in iron hydroxide sludge stabilized with cement, Environ. Sci. Technol. 37 (2003) 5050–5056.

[10] T. Phenrat, Examination of solidified and stabilized matrices of arsenic containing sludge, Masters Thesis, Inter-department Environmental management, Graduate School, Chulalongkorn University, 2004.

[11] F.M. Lea, The Chemistry of Cement and Concrete, 3rd ed., Chemical Publishing Company, New York, NY, 1970.

[12] F.P. Glasser, Chemistry of cement-solidified waste forms, in: R.D. Spence (Ed.), Chemistry and Microstructure of Solidified Waste Forms, Lewis Publishers, Ann Arbor, 1993, pp. 1–40.

[13] B. Jösson, H. Wennerström, A. Nonat, B. Cabane, Onset of cohesion in cement paste, Langmuir 20 (2004) 6702–6709.

[14] J.Y. Park, B. Batchelor, Prediction of chemical speciation in stabilized/solidified wastes using a general chemical equilibrium model II: doped waste contaminants in cement porewaters, Cem. Concr. Res. 29 (1999) 99–105.

[15] W. Stumm, J.J. Morgan, Aquatic Chemistry, 3rd ed., Wiley, New York, NY, 1996.

[16] S.C.B. Myneni, S.J. Traina, T.J. Logan, G.A. Waychunas, Oxyanion behavior in alkaline environments: sorption and desorption of arsenate in ettringite, Environ. Sci. Technol. 31 (1997) 1761–1768.

[17] S. Mindess, J.F. Young, D. Darwin, Concrete, 2nd ed., Pearson Education, Upper Saddle River, New Jersey, 2003.

[18] I. Baur, C.A. Johnson, Sorption of selenite and selenate to cement minerals, Environ. Sci. Technol. 37 (2003) 3442–3447.